

# Synthesis and characterization of square planar and pseudo-tetrahedral $M(II)N_2S_2$

Eric M. Martin and Robert D. Bereman\*

North Carolina State University, Department of Chemistry, Box 8204, Raleigh, NC 27695-8204 (U.S.A.)

(Received February 26, 1991; revised June 25, 1991)

## Abstract

Copper(II), nickel(II) and zinc(II) complexes of methyl-2-amino-1-cyclopentenedithiocarboxylate and  $N,N'$ -pentamethylene-bis(methyl-2-amino-1-cyclopentenedithiocarboxylate) have been prepared and characterized in order to provide a basis for comparison of neutral molecules involved in planar and pseudo-tetrahedral coordination geometries with similar  $N_2S_2$  ligand donor sets. Methyl-2-amino-1-cyclopentenedithiocarboxylate chelates as a bidentate ligand through a thioketonate sulfur and an imine nitrogen, forming planar complexes with the divalent ions of copper(II), nickel(II) and zinc(II). The Cu(II) complex exhibits EPR spin Hamiltonian parameters typical of an axial system with  $g_{\parallel} = 2.139$  and  $A_{\parallel} = 175 \times 10^{-4}$ .  $N,N'$ -pentamethylene-bis(methyl-2-amino-1-cyclopentenedithiocarboxylate) coordinates as a tetradentate ligand, where the pentamethylene bridge between the nitrogens introduces steric strain forcing distortion of the inner coordination sphere. Spectral data support pseudo-tetrahedral coordination geometries for both Cu(II) and Ni(II). The EPR spectrum of this Cu(II) complex is characteristic of a large tetrahedral distortion with  $g_{\parallel} = 2.146$  and  $A_{\parallel} = 133 \times 10^{-4} \text{ cm}^{-1}$ , while  $^1\text{H}$  NMR studies on the Ni(II) analogue indicate paramagnetic contact shifts of resonances, also indicative of tetrahedral distortion. The complexes are examined as possible spectral models of  $N_2S_2$  coordination environments at the active sites of metalloproteins such as in the type I blue copper(II) and nickel hydrogenase proteins.

## Introduction

Since the first report of the active site structure of a type I blue copper(II) containing protein [1, 2], there has been great interest in designing highly distorted  $M(II)N_2S_2$  systems that may serve as spectral models of the active sites of the metalloenzymes [3–5]. More recently, nickel has been discovered at the active site of several other classes of enzymes, including hydrogenases [6–9], methyl co-enzyme reductases [10] and CO dehydrogenases [11], all of which are also suggested to involve  $N_2S_2$  coordination at the metal center [12–14]. In an effort to help further understand the physical properties of these coordination environments in biological systems [15–21], we have previously synthesized and characterized a series of Cu(II) and Ni(II) complexes of a unique  $N_2S_2$  tetradentate ligand ( $n=2, 3, 4$ ) where we were able to control stepwise distortions of a constant ligand donor set from square planar to pseudo-tetrahedral geometries. This system is schematically represented in Fig. 1(a), where  $n$  equals

\*Author to whom correspondence should be addressed.

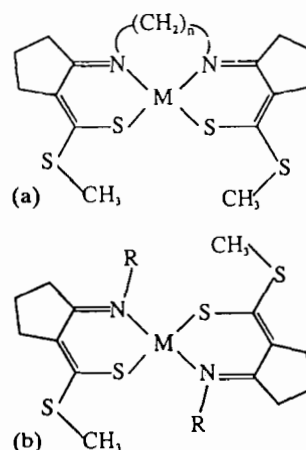


Fig. 1. (a) Lewis structure for tetradentate  $n$ -series complexes where  $n=0, 2, 3, 4$  and  $5$ . (b) Lewis structure for bis-bidentate  $R$ -series complexes, where  $R$  = methyl, ethyl,  $n$ -propyl and  $n$ -butyl.  $M(II)$  represents Cu(II), Ni(II) and Zn(II).

the number of methylene groups bridging the two 'halves' of the ligand. Here we present two new ligands, methyl-2-amino-1-cyclopentenedithiocarbox-

ylate ( $n=0$  or  $R=H$ ), shown in Fig. 1(b), and  $N,N'$ -pentamethylene-bis(methyl-2-amino-1-cyclopentenedithiocarboxylate) ( $n=5$ ), which belong to the same ligand system, and which extend the stereochemistries of the earlier series to both more planar ( $n=0$ ) and increased pseudo-tetrahedral geometries ( $n=5$ ). Coordination is through the lone pairs on the imine groups and the thioacetate sulfurs. Alkyl dithiocarboxylate functional groups diminish the difficulties involving thiol-copper(II) coordination, which frequently result in ligand oxidation by Cu(II), and the formation of Cu(I) and a disulfide [22].

Notable features of the copper(II) coordination sphere at the active site of the type I copper(II) containing proteins include a strong Cu(II)-S bond to the thiolate of a cysteine residue, a weak Cu(II)-S bond to a methionine thioether group, and two Cu(II)-N(histidine) bonds, all arranged in a low symmetry pseudo-tetrahedral environment [1, 2, 23-25]. The label 'blue' copper(II) is derived from the strong absorption in the visible spectrum near 16.6 kK ( $\epsilon=2000-5000 \text{ M}^{-1} \text{ cm}^{-1}$ ), assigned as a  $\sigma\text{S-Cu(II)}$  ligand to metal charge transfer (LMCT) band [25-27]. Anomalously low ESR parameters,  $A_{\parallel, \text{Cu}} < 100 \times 10^{-4} \text{ cm}^{-1}$  and  $A_{\parallel, \text{N}} < 8 \times 10^{-4} \text{ cm}^{-1}$  [28], are also characteristic spectral features of the copper(II) ion in the type I proteins. The proteins function as electron transfer agents [2, 29], and the catalytic cycle is thought to involve a Cu(II)/Cu(I) redox couple, which occurs at remarkably positive potentials (+180 to +780 mV versus NHE) [30-33] and is facilitated by the unusual coordination environment [25].

Information on the nickel enzymes is not nearly as detailed, due to the lack of single crystal X-ray diffraction studies. Common to many investigations of nickel metalloenzymes is the proposition of a low symmetry, four coordinate nickel active site involving nitrogen and sulfur ligand groups. Experiments using electron spin resonance, X-ray diffraction and X-ray absorption techniques suggest from one to four sulfurs bind a monomeric nickel ion at both a hydrogenase and carbon monoxide dehydrogenase active site [34-38]. Recent magnetic circular dichroism experiments have revealed the magnetic susceptibility of the nickel site in native hydrogenases is likely diamagnetic, considerably narrowing possible model geometries [39]. The catalytic properties of hydrogenase arise from the remarkably low oxidation potential for the Ni(II)/Ni(III) redox couple (-390 to -640 mV versus SCE), which enables activation of dihydrogen [34-38]. Few synthetic complexes have been able to match these low potentials, considering the typical potential for the oxidation of Ni(II) complexes lies positive of +500 mV versus SCE

[40-42]. Factors that affect the stability of trivalent Ni(III), while not well understood, normally involve ligands with different combinations of negatively charged donor atoms and coordination geometries [40-42]. Some information on Ni(II)N<sub>2</sub>S<sub>2</sub> systems with tetradentate ligands has been collected [43-56], however, a study of systematically varying stereochemistries involving Ni(II) has not been reported to our knowledge.

We, as well as others [54-63], have been interested in the relationships between the degree of tetrahedral distortion and the physical properties of Cu(II)N<sub>2</sub>S<sub>2</sub> complexes. In an effort to better understand these relationships as they pertain to both Cu(II) and Ni(II) enzymatic systems, we have extended our series [15-18] of bidentate and tetradentate [N<sub>2</sub>S<sub>2</sub>]<sup>2-</sup> ligands with flexibility that allows the attainment of neutral Cu(II) and Ni(II) complexes of both square planar and pseudo-tetrahedral coordination geometries with consistent donor sets.

## Experimental

### Materials

All reagents and solvents were commercially obtained from either Fisher Scientific or Aldrich Chemicals and used without further purification. Tetraalkylammonium salts, used as supporting electrolytes, were obtained from Southwestern Analytical Chemicals, dried for 12 h at 70 °C, and dissolved without additional recrystallization in Aldrich Gold Label solvents.

### Syntheses

#### Ligands

Methyl-2-amino-1-cyclopentenedithiocarboxylate ( $n=0$ ) and  $N,N'$ -pentamethylene-bis(methyl-2-amino-1-cyclopentenedithiocarboxylate) ( $n=5$ ) were prepared by methods previously described [64] with only slight modifications [54]. Yellow crystalline powders of each compound were isolated, analyzed for purity by elemental analyses and NMR, and used directly for subsequent reactions.

*Anal.* Calc. for C<sub>7</sub>H<sub>11</sub>N<sub>1</sub>S<sub>2</sub>: C, 48.51; H, 6.41; N, 8.08; S, 36.99. Found: C, 48.58; H, 6.44; N, 8.01; S, 36.91%.

Calc. for C<sub>19</sub>H<sub>28</sub>N<sub>2</sub>S<sub>4</sub>: C, 55.10; H, 7.25; N, 6.76; S, 30.92. Found: C, 54.93; H, 7.31; N, 6.76; S, 30.86%.

#### Metal complexes

The corresponding metal complexes of  $n=0$  were synthesized by reaction with the appropriate metal acetate in methanol [19-21, 54]. A typical reaction

involved dissolving 0.173 g (1.0 mmol) of  $n=0$  ligand in 15 ml methanol, and adding 10 ml of methanolic metal acetate (1.0 mmol). Red crystals of Cu(II)  $n=0$  were isolated directly from the reaction mixture and were somewhat unstable with respect to decomposition, probably by reduction of Cu(II) and formation of the disulfide. Green crystals of Ni(II)  $n=0$  were collected by vacuum filtration and recrystallized from dichloromethane. A yellow precipitate formed upon the reaction of the free ligand and zinc(II) acetate tetrahydrate. Analytical purity was established by elemental analyses in each case.

*Anal.* Calc. for  $\text{Cu}(\text{C}_7\text{H}_{11}\text{NS}_2)_2$ : C, 48.77; H, 5.85; N, 7.50. Found: C, 48.86; H, 5.89; N, 7.52%.

Calc. for  $\text{Ni}(\text{C}_7\text{H}_{11}\text{NS}_2)_2$ : C, 41.48; H, 4.99; N, 6.91; S, 31.66. Found: C, 41.53; H, 4.97; N, 6.91; S, 31.49%.

Calc. for  $\text{Zn}(\text{C}_7\text{H}_{11}\text{NS}_2)_2$ : C, 41.08; H, 4.89; N, 6.85; S, 31.29. Found: C, 41.14; H, 4.87; N, 6.84; S, 31.38%.

Cu(II) and Ni(II) complexes of  $n=5$  were synthesized by different methods. Cu(II)  $n=5$  was prepared by dissolving 1 equiv. of the ligand in THF and stirring in a stoichiometric amount of copper(II) acetate dissolved in absolute ethanol. After 5 min stirring at room temperature the reaction flask was placed in a dry ice/acetone bath. Precipitation of dark blue-green microcrystals occurred within 15 min. The complex exhibits stability in the solid state when exposed to the atmosphere. Ni(II)  $n=5$  was synthesized by reaction of the appropriate metal acetate and ligand in 1:1 ratios in a minimum volume of methanol. The complex was isolated from the initial filtrate by separation on a silica column with dichloromethane as the mobile phase, and recrystallized from a 70/30 dichloromethane/acetone mixture. Zn(II)  $n=5$  was prepared in a method similar to that for Ni(II)  $n=5$ .

*Anal.* Calc. for  $\text{CuC}_{19}\text{H}_{28}\text{N}_2\text{S}_4$ : C, 47.94; H, 5.89; N, 5.89. Found: C, 48.03; H, 5.94; N, 5.89%.

Calc. for  $\text{NiC}_{19}\text{H}_{28}\text{N}_2\text{S}_4$ : C, 48.41; H, 5.94; N, 5.94; S, 27.18. Found: C, 48.62; H, 6.00; N, 6.15; S, 26.98%.

Calc. for  $\text{ZnC}_{19}\text{H}_{28}\text{N}_2\text{S}_4$ : C, 47.76; H, 5.87; N, 5.87; S, 26.86. Found: C, 47.93; H, 5.92; N, 5.89; S, 26.24%.

#### Physical measurements

Electronic absorption spectra of solutions were recorded on a Cary 2300 spectrophotometer over the UV-Vis and near-IR region. The data were collected and manipulated with an Apple IIe computer.

Elemental analyses were obtained from Atlantic Microlabs, Atlanta, GA, U.S.A.

Electrochemical properties were determined in solutions of dichloromethane ( $\text{CH}_2\text{Cl}_2$ ) and dime-

thylformamide (DMF), with tetraalkylammonium perchlorate salts as supporting electrolytes, and using conventional three compartment 'H' cells. A BAS CV 27 potentiostat and YEW model 3022 A4 X-Y recorder were used in all cyclic voltammetry experiments. Measurements were made using a platinum disk working electrode and a platinum wire auxiliary electrode, with potentials referenced to a saturated calomel electrode.

NMR spectra were obtained on either a GE 500 MHz Omega FT-NMR spectrometer equipped with variable temperature apparatus, or a GE 300 MHz Omega FT-NMR instrument. All  $^1\text{H}$  spectra were obtained using  $\text{CDCl}_3$  solutions with TMS as an internal standard.

Electron spin resonance spectra were obtained on an E-3 Varian spectrometer on an evacuated quartz cold finger allowing data to be obtained at 100 K or room temperature. The magnetic field was calibrated using  $\text{VO}(\text{acac})_2$ , and  $g$  values were standardized against the absorption of diphenylpicryl hydrazine (2.003).

#### Results

The structure of the  $\text{Ni}(\text{II})\text{N}_2\text{S}_2$  complex consists of well separated, neutral monomers with a planar inner coordination geometry as predicted from spectral data. The single crystal X-ray diffraction analysis will appear in a forthcoming publication. Cu(II)  $n=0$  and Zn(II)  $n=0$  are expected to exist in similar structural arrangements.

#### Electronic absorption

The absorption maxima of the Cu(II) and Ni(II) complexes within the range from 40.0 to 7.5 kK are reported in Table 1. The remaining  $\text{N}_2\text{S}_2$  complexes of the series of tetradentate ligands are listed as well for comparison. All of the copper complexes exhibit a broad absorption of intermediate intensity in the visible region of the spectrum. The band shifts  $5300\text{ cm}^{-1}$  to lower energies, from 21.6 kK ( $\epsilon=3500\text{ M}^{-1}\text{ cm}^{-1}$ ) in Cu  $n=0$  to 16.3 kK ( $\epsilon=2500\text{ M}^{-1}\text{ cm}^{-1}$ ) in Cu  $n=5$ . A significant red shift is also noted for the observable d-d transition. The ligand field band shifts  $4900\text{ cm}^{-1}$  from 13.2 kK ( $\epsilon=70\text{ M}^{-1}\text{ cm}^{-1}$ ) in Cu  $n=0$  to 8.3 kK ( $\epsilon=20\text{ M}^{-1}\text{ cm}^{-1}$ ) for Cu  $n=5$ . Solvent dependence is small and coordination by DMF is discounted by the similarity of the spectrum of the solid and solution. Interestingly, Cu  $n=5$  shows a slightly lower visible absorption band in the solid state as compared to the solution energies. The transition occurring at 16.3 kK shifts to 15.2 kK in the nujol mull spectrum. Decomposition prevented obtainment of the solid

TABLE 1. Electronic absorption spectral features for Ni(II) and Cu(II),  $n=0-5$ 

Complex	$\lambda_{\max}$ ( $10^3 \text{ cm}^{-1}$ ) ( $\epsilon$ ( $\text{M}^{-1} \text{ cm}^{-1}$ ))
Cu $n=0$	34.4(26000); 28.9(32000); 25.4(16000); 21.6(3500)
Cu $n=2$	34.0(25000); 31.6(33000); 28.9(15000); 26.5(16000); 25.1(sh); 20.6(sh); 12.6(70)
Cu $n=3$	34.5(26000); 26.2(14000); 24.9(15000); 20.5(3300); 17.9(sh); 10.5(6)
Cu $n=4$	38.5(32000); 30.9(34000); 30.8(31000); 26.1(1200); 25.0(sh); 18.4(3000); 9.1(20)
Cu $n=5$	34.5(30000); 29.0(26000); 26.0(16000); 16.3(2500); 8.3(20)
Ni $n=0$	37.9(34000); 30.3(28000); 28.1(21000); 24.0(10000); 22.7(15000); 21.1(4000); 15.7(30)
Ni $n=2$	30.0(28000); 28.1(16500); 23.8(4500); 22.6(6500); 21.1(4000); 15.2(130)
Ni $n=3$	30.4(30000); 26.9(9000); 24.7(5000); 22.1(6000); 14.9(170)
Ni $n=4$	38.5(36000); 30.3(28000); 26.5(6000); 21.8(4000); 14.8(200)
Ni $n=5$	38.0(28000); 29.5(24000); 26.3(7500); 20.8(4000); 14.4(200)

All spectral data reported for  $\text{CH}_2\text{Cl}_2$  solutions.

state, nujol mull spectrum of Cu  $n=0$ . Both Cu  $n=0$  and Cu  $n=5$  were unstable in solution over short periods of time, undoubtedly due to instability of the Cu-S bond in this system.

The spectrum of Ni  $n=0$  reveals three charge transfer (CT) bands narrowly spaced within the region between 24.0 and 21.1 kK, similar to Ni  $n=2$ , and assigned to  $\sigma$ - and  $\pi$ S-Ni(II) transitions. Bridging two  $n=0$  ligands to form the tetradentate complexes causes the three bands to collapse into a broad band which red shifts with increasing tetrahedral distortion. The spectrum for Ni  $n=5$  presents the lowest CT absorption energy within the series. The ligand field transitions of the Ni(II) series also show a marked dependence on bridge length, or coordination geometry, red shifting  $1300 \text{ cm}^{-1}$  from 15.7 kK ( $\epsilon=30 \times 10^{-4} \text{ cm}^{-1}$ ) for Ni  $n=0$  to 14.4 kK ( $\epsilon=200 \times 10^{-4} \text{ cm}^{-1}$ ) for Ni  $n=5$ . The increase in  $\epsilon$  is expected, due to the loss of inversion center in the *cis*, bridged complexes. Little dependence on solvent is apparent for all the nickel(II) complexes. Table 2 lists absorption maxima in different solvents for only the lowest energy charge transfers and observable ligand field transitions.

### Electrochemistry

Potentials for reductive and oxidative electrochemical processes are given in Table 3. Each Cu(II) complex exhibits a reversible one electron reduction typical of a Cu(II)/Cu(I) redox process. Analysis of integrated peak intensities and peak to peak separations at various scan rates confirms a one electron,

reversible reduction. Both Cu  $n=0$  and Cu  $n=5$  show irreversible oxidations with distantly coupled reduction processes, indicating a complicated electron transfer-chemical reaction mechanism (ECE mechanism). A second irreversible oxidation potential indicates oxidation of the ligand and loss of the starting material. Performing the experiments in coordinating and non-coordinating solvents verified strictly four coordinate solution stereochemistries.

The values for Ni  $n=0$  and Ni  $n=5$  voltammetric responses fit well into the trends of the reduction and oxidation potentials determined for Ni  $n=2, 3$  and 4. The planar Ni  $n=0$  is both more difficult to oxidize and more difficult to reduce, while Ni  $n=5$  is the least energetically demanding. The reversibility of the reductions was checked by scanning at various rates, and examining the ratio of cathodic to anodic current. Comparisons to the electrochemistry of the free ligands and analogous Zn(II) complexes indicated ligand reduction and oxidation values beyond the potentials observed for the Ni(II) complexes, supporting metal based reductions and oxidations. Complicated oxidation processes led to large  $i_{p,a}/i_{p,c}$  ratios and  $\Delta E_p$  values, suggesting stereochemical rearrangement and possible decomposition of the starting sample.

### Electron spin resonance

X-band ESR spectra were obtained of solutions and glasses containing the two Cu(II) complexes, and spin Hamiltonian parameters are reported in Table 4. Frozen glass spectra in both coordinating (DMF/ $\text{CH}_2\text{Cl}_2$ ) and non-coordinating (toluene/ $\text{CH}_2\text{Cl}_2$ ) solvent mixtures show similar spectral values consistent with four coordinate geometries. The solution spectrum of Cu  $n=0$  in toluene is shown in Fig. 2 and shows well resolved five line fine structure indicating coordination to two equivalent nitrogens. The spectrum of Cu  $n=0$  in a frozen glass of toluene/ $\text{CH}_2\text{Cl}_2$ , shown in Fig. 3, indicates spin Hamiltonian parameters characteristic of an axially symmetrical system with  $g_{\parallel}=2.128(2)$  greater than  $g_{\perp}=2.037(2)$ . Well resolved nitrogen superhyperfine splitting reveals five lines in both the parallel and perpendicular regions, with  $A_{\parallel,\text{Cu}}=166.2(5) \times 10^{-4} \text{ cm}^{-1}$ ,  $A_{\parallel,\text{N}}=11.9(5) \times 10^{-4} \text{ cm}^{-1}$  and  $A_{\perp,\text{N}}=14.2(5) \times 10^{-4} \text{ cm}^{-1}$ . The spectrum for Cu  $n=5$  in a frozen glass of 1:1 toluene/ $\text{CH}_2\text{Cl}_2$  is shown in Fig. 4. The spectrum is typical of a rhombic environment around the Cu(II) ion, with  $g_{zz} > g_{xx} \sim g_{yy}$ , and the  $d_{x^2-y^2}$  ground state. Fine structure within the perpendicular region of the spectrum (12 G) is probably due to nitrogen superhyperfine splitting of the  $g_{xx}$  and  $g_{yy}$  components. Weak nitrogen splitting of low resolution is also observed on the four ( $A_{\parallel}=133 \times 10^{-4} \text{ cm}^{-1}$ ) line

TABLE 2. Selected electronic absorption ( $\pm 0.1 \times 10^3 \text{ cm}^{-1}$ ) maxima for  $\text{N}_2\text{S}_2$  complexes

Complex	$\text{CH}_2\text{Cl}_2$		DMF		Nujol	
	LMCT	d-d	LMCT	d-d	LMCT	d-d
Cu $n=0^a$	21.6	13.2	21.8	13.1		
Cu $n=2$	20.6	12.6	21.0	12.6		12.5
Cu $n=3$	20.5	10.5	20.5	10.5		10.5
Cu $n=4$	18.4	9.1	18.5	9.3		9.1
Cu $n=5$	16.3	8.3	16.3	8.3	15.2	8.2
Ni $n=0$	22.7	15.7	22.7	15.7	22.1	15.6
Ni $n=2$	22.6	15.2	22.6	15.2	22.0	15.1
Ni $n=3$	22.1	14.9	22.2	14.9	21.9	15.0
Ni $n=4$	21.8	14.8	21.8	14.7	20.8	14.6
Ni $n=5$	20.8	14.4	20.8	14.4	20.6	14.3

<sup>a</sup>Decomposes in the solid state.

TABLE 3. Cyclic voltammetry responses of Cu(II) and Ni(II) $\text{N}_2\text{S}_2$  complexes in DMF solutions

Complex	$E_{\text{ox}}$	$E_{1/2, \text{red}}$
Cu $n=0$	520(60)	-790(70)
Cu $n=2$	530(75)	-1010(74)
Cu $n=3$	580 <sub>i</sub>	-790(65)
Cu $n=4$	700 <sub>i</sub>	-640(70)
Cu $n=5$	725 <sub>i</sub>	-525(65)
Ni $n=0$	800 <sub>i</sub>	-1590(65)
Ni $n=2$	750 <sub>i</sub>	-1540(70)
Ni $n=3$	680 <sub>i</sub>	-1430(70)
Ni $n=4$	590 <sub>i</sub>	-1270(70)
Ni $n=5$	575 <sub>i</sub>	-1220(70)

0.1 mM solutions with 0.1 M TEAP as supporting electrolyte. Values in parentheses represent  $\Delta E_p = E_{p,c} - E_{p,a}$  i = irreversible 200 mV/s scan rate at room temperature.

TABLE 4. Electron spin resonance parameters for Cu(II) $\text{N}_2\text{S}_2$  series. Microwave frequency 9.1 GHz (X band)

Complex	$g_o^a$	$A_o^a$	$g_{\parallel}^b$	$A_{\parallel}^b$	$A_{\parallel, N}^b$
Cu $n=0^c$	2.070	79.9	2.128	166	11.9
Cu $n=2$	2.055	81.1	2.117	181	13.2
Cu $n=3$	2.060	65.3	2.132	160	12.0
Cu $n=4$	2.066	55.9	2.140	145	9.1
Cu $n=5$	2.085	65.2	2.157	133	9.0

<sup>a</sup>Ambient temperature,  $\text{CH}_2\text{Cl}_2/\text{DMF}$  50/50 by vol. solvent mixture. All hyperfine values reported  $\pm 0.5 \times 10^{-4} \text{ cm}^{-1}$ .  $g$  values  $\pm 0.002$ . <sup>b</sup>Frozen glass spectra at 100 K,  $\text{CH}_2\text{Cl}_2/\text{DMF}$  50/50 by vol. solvent mixture. Coordination by solvent molecules was checked by using toluene or  $\text{CH}_2\text{Cl}_2$ /toluene solutions and glasses. DPPH was used as a standard ( $g=2.003$ ). <sup>c</sup>Unstable in solution at elevated temperatures.

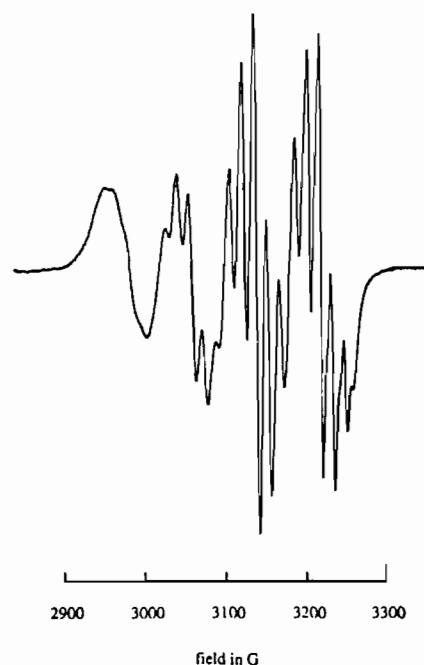


Fig. 2. ESR spectrum of Cu  $n=0$  as a solution in 60/40 toluene/ $\text{CH}_2\text{Cl}_2$  mixture. Microwave frequency 9.118 GHz (X band).

parallel pattern of Cu(II). The ESR parameters for Cu  $n=5$  indicate a completion of the trend from Cu  $n=2$  to Cu  $n=4$ , showing larger  $g_{\parallel}$  values and smaller  $A_{\parallel}$  parameters.

#### Nuclear magnetic resonance

The  $^1\text{H}$  NMR spectral features of the free ligands, Zn(II) complexes and Ni(II) complexes are reported in Table 5. Disappearance of the NH peak shifted furthest downfield provided evidence of chelation in each of the metal complexes. Small shifts in proton resonances in the Zn(II) complexes are attributed

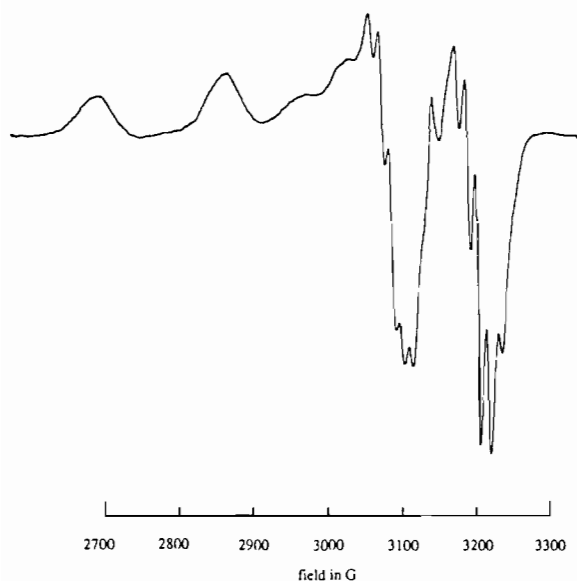


Fig. 3. ESR spectrum of Cu  $n=0$  in a frozen glass of 60/40 toluene/ $\text{CH}_2\text{Cl}_2$ . Microwave frequency 9.118 GHz (X band).

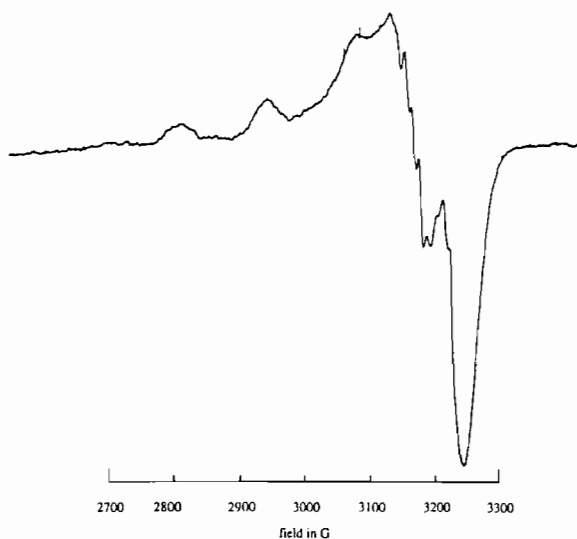


Fig. 4. ESR spectrum of Cu  $n=5$  in a frozen glass of 60/40 toluene/ $\text{CH}_2\text{Cl}_2$ . Microwave frequency 9.118 GHz (X band).

to slight changes in electronic structure accompanying chelation by the ligand. The Zn(II) species were utilized as diamagnetic reference molecules for the resonances of the Ni(II) analogues. The NMR spectrum of Ni  $n=0$  shows only small shifts from the respective Zn  $n=0$  proton resonances. Ni  $n=5$  on the other hand reveals significant shifts in resonances when compared to the diamagnetic Zn(II) reference. Protons attached to the nitrogens show the largest downfield shifts of nearly 3.2 ppm at room temperature. As the temperature is raised the N- $\text{CH}_2$ ,

5- $\text{CH}_2$  and 7- $\text{CH}_2$  resonances shift proportionally with the increases, consistent with a similar pattern observed for Ni  $n=4$  [20]. The N- $\text{CH}_2$  proton resonance shifts downfield along with the triplet from 7- $\text{CH}_2$ , while the triplet from 5- $\text{CH}_2$  moves upfield.

## Discussion

The complexes of the  $n=0$  and  $n=5$  ligands serve to complete the series of  $\text{N}_2\text{S}_2$  complexes we reported earlier [15–21]. Methyl-2-amino-1-cyclopentenedithiocarboxylate ( $n=0$ ), the starting material for the synthesis of the bridged ligands, is a strong chelating agent and stabilizes planar structures of Cu(II), Ni(II) and Zn(II). When two of these moieties are bridged together via a methylene backbone connecting the coordinating nitrogens, steric hindrance is introduced which forces the inner coordination sphere to twist from square planar to pseudo-tetrahedral geometries. The most convenient way to refer to the inner coordination sphere distortion angle for  $\text{N}_2\text{S}_2$  complexes is to define the twist, or dihedral, angle ( $\phi$ ) as the angle formed by the intersection of the M(II)SS' and M(II)NN' planes. Four coordinate molecules can vary from square planar,  $\phi=0^\circ$ , to tetrahedral,  $\phi=90^\circ$ , stereochemistries. The M(II)  $n=0$  complexes have rigid square planar inner coordination sphere geometries, and thus stand as a convenient point for comparisons to molecules of varying degrees of tetrahedral distortion.

Few examples of changing coordination environment with simultaneous conservation of ligand donor have appeared in the literature [15–21, 57–63]. Recent work from one laboratory involves Cu(II) $\text{N}_2\text{S}_2$  coordination by a non-symmetric collection of donor atoms in a tetradentate ligand system [60–63]. Variation of the size of two chelating rings leads to tetrahedral distortion and the stabilization of five coordinate and four coordinate cationic species [60–62]. More commonly, the length of a single carbon chain bridging symmetrical halves of a ligand has been varied in order to induce geometrical changes at the metal [53–59]. The Cu(II) and Ni(II)  $n=0$  through  $n=5$  complexes involve a similar method of distortion and result in the highly distorted M(II)  $n=5$  molecules, of which Cu  $n=5$  exhibits physical properties approaching those of the blue protein active sites.

Figure 5 shows the classical  $g_{\parallel}$  versus  $A_{\parallel}$  map developed by Blumberg and Piesach [65] with two type I blue copper proteins and the Cu  $n=0$ –5 series included. At the time of inception of the relationship, it was reasoned that increased tetrahedral distortion of the inner coordination sphere would force the  $g$  value to become larger, but at a slower pace than

TABLE 5.  $^1\text{H}$  NMR resonances ( $\pm 0.005$  ppm) of the free ligands and Ni(II) and Zn(II) $\text{N}_2\text{S}_2$  complexes

Compound	Protons							
	1-CH <sub>3</sub>	5-CH <sub>2</sub>	6-CH <sub>2</sub>	7-CH <sub>2</sub>	8-CH <sub>2</sub>	9-CH <sub>2</sub>	9-CH <sub>2</sub>	7-NH
L $\text{N}_2\text{S}_2$ $n=0$	2.591	2.634	1.882	2.827				5.706, 11.252
Zn $\text{N}_2\text{S}_2$ $n=0$	2.591	2.627	1.776	2.739				7.236
Ni $\text{N}_2\text{S}_2$ $n=0$	2.644	2.398	1.812	2.632				5.233
L $\text{N}_2\text{S}_2$ $n=2$	2.593	2.710	1.837	2.800	3.632			12.42
Zn $\text{N}_2\text{S}_2$ $n=2$	2.598	2.714	1.943	2.807	3.528			
Ni $\text{N}_2\text{S}_2$ $n=2$	2.622	2.562	1.876	2.620	3.354			
L $\text{N}_2\text{S}_2$ $n=3$	2.593	2.715	2.029	2.815	3.567	1.890		12.42
Zn $\text{N}_2\text{S}_2$ $n=3$	2.598	2.722	1.950	2.822	3.586	1.898		
Ni $\text{N}_2\text{S}_2$ $n=3$	2.595	2.515	1.873	2.617	3.640	1.861		
L $\text{N}_2\text{S}_2$ $n=4$	2.598	2.703	1.895	2.820	3.340	1.822		12.42
Zn $\text{N}_2\text{S}_2$ $n=4$	2.603	2.720	2.037	2.820	3.564	1.898		
Ni $\text{N}_2\text{S}_2$ $n=4$	2.595	2.144	1.820	3.142	5.043	1.742		
L $\text{N}_2\text{S}_2$ $n=5$	2.598	2.698	1.895	2.818	3.339	1.720	1.573	12.42
Zn $\text{N}_2\text{S}_2$ $n=5$	2.600	2.723	2.041	2.820	3.564	1.718	1.596	
Ni $\text{N}_2\text{S}_2$ $n=5$	2.576	2.140	1.700	3.247	6.502	1.010	1.827	

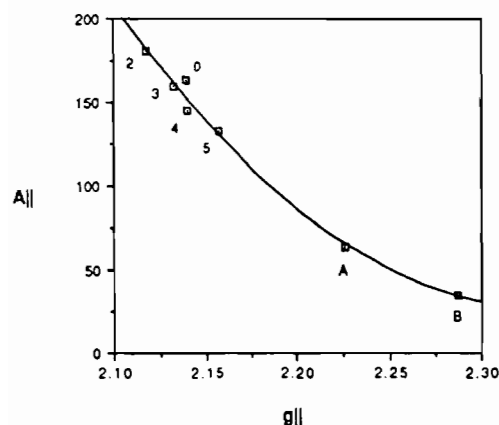


Fig. 5. Plot of  $A_{||}$  vs.  $g_{||}$  for  $\text{Cu(II)N}_2\text{S}_2$   $n$ -series ( $n=0, 2, 3, 4$  and  $5$ ) and type I blue protein  $\text{Cu(II)}$  active sites (A = stellacyanin; B = plastocyanin).

the decreasing  $A_{||}$  value, causing the point to drop to the lower left of the map. Indeed, this is the case. The  $A_{||}$  value for  $\text{Cu } n=5$ ,  $133 \times 10^{-4} \text{ cm}^{-1}$ , is one of the lowest values for any stable, neutral  $\text{Cu(II)N}_2\text{S}_2$  complex yet reported [15–18, 21, 52, 66]. Similar hyperfine splitting values are reported for a pyridine thiolate cationic complex [5], and bidentate  $N$ -substituted  $\beta$ -aminothiones [66]. The  $g_{||}$  value of 2.157 and  $g_{\perp}$  value of 2.057 for  $\text{Cu } n=5$  are consistent with other similar pseudo-tetrahedral type complexes of heterocyclic thiols [21, 52, 66].

Extrapolation of experimental data suggests that the  $\text{Cu } n=5$  complex maintains a dihedral angle slightly larger than  $60^\circ$ . A nearly linear relationship exists between any of the spectral values and  $\phi$ . Both  $\text{Cu } n=0$  and  $\text{Cu } n=5$  fall on the lines established

by relationships between ligand field transition energies and  $\phi$ , hyperfine coupling constants and  $\phi$ , and redox potentials and  $\phi$ . A non-linear relationship between  $g_{||}$  and  $\phi$  is expected [26, 67], where the slope is much larger when angles increase to values over  $60^\circ$ .

The charge transfer band of  $\text{Cu } n=5$  at 16.3 kK corresponds well with the values for  $\sigma\text{S-Cu(II)}$  LMCTs found in the native blue proteins [26]. The broad, intense band is probably due to combinations of  $\sigma$  and  $\pi\text{S-Cu(II)}$  charge transfers, all broadened by interactions with  $\text{S-Cu}$  vibrations. Assignment of the 16.3 kK band to a LMCT band is consistent with the observed large  $\epsilon$ , the expected distortion of the complex, and the smooth progression of the band through the  $n$ -series as a function of dihedral angle. A progression of the band from a position of higher energy in the planar  $n=0$  complex can be traced, and the corresponding CT transition energy maximum for each of the  $\text{CuN}_2\text{S}_2$  complexes is collected in Table 2. X-ray crystallography of the  $\text{Cu(II)}$  [15–18] and  $\text{Ni(II)}$  [20]  $n=2, 3$  and  $4$  complexes suggests the  $\text{M(II)-S}$  bond lengths decreases as a function of dihedral angle, owing to greater orbital overlap between the empty  $d\pi$  S and filled  $d\pi$   $\text{Cu(II)}$  atomic orbitals, and less S-S steric crowding. EHMO calculations on  $\text{CuN}_2\text{S}_2$  model complexes similar to  $\text{Cu } n=4$  concluded that the spin density on the  $\text{Cu } 3d$  decreased as a function of  $\phi$ , indicating increased  $\text{Cu-S}$  bond covalency which contributes to lower energy  $\text{S-Cu}$  charge transfers [18]. Two low energy LMCTs are reported for a similar compound with copper(II) thiolate chromophore and  $59.1^\circ$  dihedral

angle [57]. Absorption bands at 18.7 and 15.2 ( $\epsilon = 3000$  and  $1500 \text{ M}^{-1} \text{ cm}^{-1}$ ) were assigned to  $\sigma\text{S-Cu(II)}$  and  $\pi\text{S-Cu(II)}$  transitions, respectively [57]. Two low energy charge transfers of comparable positions are also reported for complexes of N-substituted  $\beta$ -aminothiones [66]. Cu  $n = 5$  exhibits a band at 16.3 kK in both dichloromethane and DMF, and at 15.2 kK in the solid state as a mull of nujol oil. The discrepancy between solution and solid state values suggests that the solid state molecular structure may reveal stabilization of  $\phi > 65^\circ$ .

Generally a red shift is also expected for ligand field transition energies as the geometry changes from  $D_{4h} \rightarrow D_{2d} \rightarrow T_d$ . Using the technique outlined by Companion and Komarynski to predict the d-d transitions for Cu(II) $\text{N}_2\text{S}_2$  environments [68] the lowest ligand field transition energy for Cu  $n = 5$  of 8.3 kK corresponds to a twist angle of approximately  $65^\circ$ . The value of 8.3 kK is also consistent with the trend seen in the previous four Cu(II) complexes of the series, and correlates well with the d-d band found between 8–12 kK for the type I sites in metalloenzymes [26, 27].

The redox potentials of Cu  $n = 5$ , which also show a continuation of the trend earlier established, still remain distant from the values for the biological systems. The coordination geometry only represents a portion of the factors which influence the thermodynamic redox process [69]. The type of donor atom seems to play a more important role, yet, it is instructive to note the role that coordination geometry plays in stabilizing oxidation states in the present system where consistency of donor type is maintained. The anomalous value for the reduction of Cu  $n = 0$  is considered a result of *trans* rather than *cis* bonding configuration.

The Ni(II)  $\text{N}_2\text{S}_2$  complexes are interesting in light of the continuing interest in the bioinorganic chemistry of nickel, and its use in metal substitution studies of blue copper proteins [70–74]. The structure of Ni  $n = 0$  represents the most stable electronic environment for Ni(II) in the series, combining *trans* coordination and square planar environment. Ligands containing sulfur donor atoms generally show preference for planar stereochemistries with  $d^8$  ions, and the majority of other synthetic Ni(II) $\text{N}_2\text{S}_2$  complexes prepared are indeed square planar [75–78]. Recent work has involved the preparation of negatively charged square planar complexes of ligand types that may help stabilize trivalent nickel [47, 79–82]. A highly anionic  $[\text{Ni(II)N}_2\text{S}_2]^{2-}$  complex was produced which exhibited very low values for the Ni(II)/Ni(III) redox couple [47]. Although the present ligands do not exhibit such low redox potentials, it is again valuable to note the effects changing coordination

environment have on electrochemical properties. Changing from planar Ni  $n = 0$  to pseudo-tetrahedral Ni  $n = 5$  involves a change in oxidation potential of 250 mV, and in reduction potential of 410 mV. It quickly becomes apparent that increased distortion of an  $[\text{Ni(II)N}_2\text{S}_2]^{2-}$  environment from square planar to tetrahedral geometries could have a large influence upon the already low oxidation potentials.

Substitution of Ni(II) into blue copper active sites allows spectroscopic analyses unavailable with Cu(II), which aid in structural characterizations [71] and provide evidence for the argument of whether the rigid protein fold constrains the coordination geometry, independent of the central metal ion [73]. It has been shown that at least one Ni(II) derivative of a native Cu(II) enzyme absorbs in the near IR region [71, 72], characteristic of tetrahedral, or pseudo-tetrahedral,  $d^8$  symmetries. Ni(II) substituted azurin exhibits a strong absorbance near 22.8 kK assigned to a LMCT  $\pi\text{S-Ni(II)}$  transition, corresponding to the band near 16.0 kK in the native copper(II) containing proteins [70–74]. A similar pattern occurs when changing metals with the present  $n$ -series of ligands. The shift between Cu  $n = 5$  absorption maximum, 16.3 kK, and Ni  $n = 5$  absorption maximum, 20.8 kK, reveals a  $4500 \text{ cm}^{-1}$  shift comparable to the  $4800 \text{ cm}^{-1}$  shift from Cu(II) to Ni(II) azurin. The discrepancy is likely due to the lesser degree of distortion expected in the Ni(II) complex (see Table 2), and suggests that the metal does play a role in the geometry of the active site.

In solution, four coordinate Ni(II) complexes are prone to exhibit equilibrium between planar and tetrahedral stereochemistries resulting in a ground state with triplet character. Paramagnetic Ni(II) causes spin polarization of ligand orbitals, shifting ligand proton resonances from their normal values in diamagnetic environments. Many well studied examples involve ligand types incorporating delocalized  $\pi$ -systems [83–87]. There are two classifications of interactions with paramagnetic ions which affect nuclear resonances: contact, or through bond interactions, and dipolar interactions. The nature of the observed shifts for Ni  $n = 5$  indicate they arise from a Fermi contact mechanism which delocalizes odd spin through the ligand orbitals [88]. Dipolar shifts arise from through space interactions and are normally considered negligible for systems similar to the present series of compounds. Since the shifts exhibit a linear relationship with temperature, the following relationship holds true [83]:

$$\Delta f_o/f_i = -a_i(g_e/g_H)\{[\beta g S(S+1)]/6SkT\} \times [\exp(-\Delta G/RT) + 1]^{-1} \quad (1)$$



In (1)  $\Delta f_0$  is the difference, or shift, in resonance for any given proton between analogous diamagnetic and paramagnetic molecules,  $f_i$  is the frequency of the NMR instrument,  $a_i$  is the electron-nuclear hyperfine coupling constant in Gauss, and  $g$  is the  $g$  value of the paramagnetic form. The remaining symbols have their usual meanings. The bracketed exponential term,  $[\exp(-\Delta G/RT) + 1]^{-1}$ , represents  $N_p$ , the fraction of paramagnetic character of the sample in solution at temperature,  $T$ , or the fractional proportion of twist in the inner coordination sphere from square planar to tetrahedral geometry. Zinc(II) derivatives were used as diamagnetic references.

Obtaining the shift values for the protons of 5-CH<sub>2</sub> and 7-CH<sub>2</sub>, and  $a_i$  values imported from a suitable tetrahedral, paramagnetic compound [83], an average value for  $N_p$  was calculated for the Ni  $n=5$  sample at 22°.  $N_p$  calculated for Ni  $n=4$  was approximately 3% [19], a small value considering the dihedral angle between the NiNN' and NiSS' planes was 36°. Ni  $n=5$  exhibits only slightly larger shifts at 22°, resulting in  $N_p \sim 4\%$ . Similar bis-bidentate NiN<sub>2</sub>S<sub>2</sub> complexes show much larger shifts, or at least sensitivity to the paramagnetic influence [21]. An interesting correlation can be made between the magnitude of paramagnetic NMR shifts for the Ni(II) complexes and the spectral data for the Cu(II) complexes. Both ESR  $A_{\parallel}$  hyperfine splitting parameters and Fermi contact shift magnitudes are dependent upon the amount of S-M(II) orbital overlap, or extent of S-M(II) covalency. Lower  $A_{\parallel}$  parameters and larger paramagnetic shift magnitudes both support the same conclusion, therefore, that systematically induced tetrahedral distortion results in greater S-M(II) covalency.

## Conclusions

A series of four coordinate Cu(II) and Ni(II) complexes that include both square planar and highly distorted pseudo-tetrahedral molecules has been completed. Spectral data indicate a Cu(II)N<sub>2</sub>S<sub>2</sub> chromophore similar to that of the blue copper proteins results from distortion of the inner coordination to pseudo-tetrahedral geometries. A S-Cu(II) CT absorbance at 16.3 kK represents one of the lowest yet achieved for synthetic Cu(II)N<sub>2</sub>S<sub>2</sub> complexes. High  $g_{\parallel}$  (2.157) and low  $A_{\parallel}$  ( $133 \times 10^{-4} \text{ cm}^{-1}$ ) ESR spin Hamiltonian parameters obtained from frozen glass spectra also indicate significant tetrahedral distortion.

Similar, stepwise distortions in the coordination environment occur for the analogous Ni(II)N<sub>2</sub>S<sub>2</sub> complexes. Ni  $n=0$  through  $n=5$  are now reported,

indicating lower oxidation potentials and ligand to metal charge transfer energies can be achieved through tetrahedral distortion of the inner coordination environment of Ni(II). Nevertheless, the present complexes still involve a large overpotential when compared to the Ni(II)/Ni(III) couples in native metalloenzymes.

## References

- 1 P. M. Colman, H. C. Freeman, J. M. Guss, M. Murata, V. A. Norris, J. A. M. Ramshaw and M. P. Venkatappa, *Nature (London)*, 272 (1978) 319.
- 2 J. M. Guss and H. C. Freeman, *J. Mol. Biol.*, 169 (1983) 521.
- 3 K. D. Karlin and J. Zubieta (eds.), *Copper Coordination Chemistry: Biochemical and Bioinorganic Perspectives*, Vols. I and II, Adenine, New York, 1982.
- 4 T. G. Spiro (ed.), *Copper Proteins*, Wiley, New York, 1981.
- 5 H. Toftlund, J. Becher, P. H. Oleson and J. Z. Pederson, *Isr. J. Chem.*, 25 (1985) 56.
- 6 J. J. G. Moura, M. Teixeira, I. Moura, A. V. Xavier and J. LeGall, *J. Mol. Catal.*, 23 (1984) 303.
- 7 R. D. Cammack, D. O. Hall and K. K. Rao, in R. K. Poole and C. Dow (eds.), *Microbial Gas Metabolism; Mechanistic, Metabolic and Biotechnological Aspects*, Academic Press, New York, 1985, pp. 75-102.
- 8 E.-G. Graf and R. K. Thauer, *FEBS Lett.*, 136 (1981) 165.
- 9 R. D. Cammack, D. Patil, R. Aguirre and E. C. Hatchikian, *FEBS Lett.*, 142 (1982) 289.
- 10 S. W. Ragsdale, L. G. Ljungdahl and D. V. DerVartanian, *Biochem. Biophys. Res. Commun.*, 115 (1983) 658.
- 11 S. W. Ragsdale, H. G. Wood and W. E. Antholine, *Proc. Natl. Acad. Sci. U.S.A.*, 82 (1985) 6811.
- 12 R. P. Hausinger, *Microbiol. Rev.*, 51 (1987) 22.
- 13 R. Cammack, *Adv. Inorg. Chem.*, 32 (1988) 297.
- 14 J. Lancaster (ed.), *The Bioinorganic Chemistry of Nickel*, VCH, New York, 1988.
- 15 R. D. Bereman, M. W. Churchill and G. D. Shields, *Inorg. Chem.*, 18 (1979) 3117.
- 16 R. D. Bereman, G. D. Shields, J. Bordner and J. R. Dorfman, *Inorg. Chem.*, 20 (1981) 2165.
- 17 R. D. Bereman, J. R. Dorfman, J. Bordner, P. Rilemma, P. McCarthy and G. D. Shields, *J. Bioinorg. Chem.*, (1982) 49.
- 18 R. D. Bereman, J. R. Dorfman and M.-H. Whangbo, in K. D. Karlin and J. Zubieta (eds.), *Copper Coordination Chemistry: Biochemical and Bioinorganic Perspectives*, Vol. I, Adenine, New York, p. 75.
- 19 E. M. Martin, R. D. Bereman and J. R. Dorfman, *Inorg. Chim. Acta*, 176 (1990) 247.
- 20 E. M. Martin, R. D. Bereman and P. Singh, submitted for publication.
- 21 E. M. Martin and R. D. Bereman, submitted for publication.
- 22 C. G. Kuehn and S. S. Isied, *Prog. Inorg. Chem.*, 27 (1979) 153.

- 23 G. E. Norris, B. F. Anderson and E. N. Baker, *J. Am. Chem. Soc.*, **108** (1986) 2784.
- 24 E. T. Adman and L. H. Jensen, *Isr. J. Chem.*, **21** (1981) 8.
- 25 D. R. McMillin, *J. Chem. Educ.*, **62** (1985) 997, and refs. therein.
- 26 E. I. Solomon, J. W. Hare, D. M. Dooley, J. H. Dawson, P. J. Stephens and H. B. Gray, *J. Am. Chem. Soc.*, **102** (1980) 168.
- 27 K. W. Penfield, R. R. Gay, R. S. Himmelwright, N. C. Eickman, V. A. Norris, H. C. Freeman and E. I. Solomon, *J. Am. Chem. Soc.*, **103** (1981) 4382.
- 28 B. G. Malmstrom and T. J. Vanngard, *J. Mol. Biol.*, **2** (1960) 118.
- 29 O. Farver and I. Pecht, in R. Lontie (ed.), *Copper Proteins and Copper Enzymes*, Vol. I, CRC Press, Boca Raton, FL, 1984, p. 157.
- 30 B. Reinhammar and B. G. Malmstrom, in T. G. Spiro (ed.), *Copper Proteins*, Wiley, New York, 1981, p. 109.
- 31 T. Sakurai, K. Okamoto, K. Kawahara and A. Nakahara, *FEBS Lett.*, **147** (1982) 220.
- 32 K. O. Burkey and E. Gross, *Biochemistry*, **20** (1981) 5495.
- 33 V. T. Taniguchi, B. G. Malmstrom, F. C. Anson and H. B. Gray, *Proc. Natl. Acad. Sci., U.S.A.*, **79** (1982) 3387.
- 34 D. V. DerVartanian, H.-J. Krüger, H. D. Peck, Jr. and J. LeGall, *Rev. Port. Quim.*, **27** (1975) 70.
- 35 S. P. J. Albracht, A. Kroger, J. W. Van der Zwaan, G. Uden, R. Bocher, H. Mell and R. D. Fontijn, *Biochim. Biophys. Acta*, **874** (1986) 116.
- 36 P. A. Lindahl, N. Kojima, R. P. Hausinger, J. A. Fox, B. K. Teo, C. T. Walsh and W. H. Orme-Johnson, *J. Am. Chem. Soc.*, **106** (1984) 3062.
- 37 R. A. Scott, S. A. Wallin, M. Czechowski, D. V. DerVartanian, J. LeGall, H. D. Peck Jr. and I. Moura, *J. Am. Chem. Soc.*, **106** (1984) 6864.
- 38 S. P. Cramer, M. K. Eidsness, W.-H. Pan, T. A. Morton, S. W. Ragsdale, D. V. DerVartanian, L. G. Ljungdahl and R. A. Scott, *Inorg. Chem.*, **26** (1987) 2477.
- 39 A. T. Kowal, I. C. Zambrano, I. Moura, J. J. G. Moura, J. LeGall and M. K. Johnson, *Inorg. Chem.*, **27** (1988) 1162.
- 40 K. Nag and A. Chakravorty, *Coord. Chem. Rev.*, **33** (1980) 87.
- 41 R. J. Haines and A. McAuley, *Coord. Chem. Rev.*, **39** (1981) 77.
- 42 A. G. Lappin and A. McAuley, *Adv. Inorg. Chem.*, **32** (1988) 241.
- 43 L. F. Lindoy and R. J. Smith, *J. Inorg. Chem.*, **20** (1981) 1314.
- 44 L. A. Drummond, K. Henrick, M. J. L. Kangasundaram, L. F. Lindoy, M. McPartlin and P. A. Tasker, *Inorg. Chem.*, **21** (1982) 2963.
- 45 J. W. L. Martin, G. J. Organ, K. P. Wainwright, K. D. V. Weerasuria, A. C. Willis and S. B. Wild, *Inorg. Chem.*, **28** (1987) 4531.
- 46 P. A. Duckworth, F. S. Stephens, K. P. Wainwright, K. D. V. Weerasuria and S. B. Wild, *Inorg. Chem.*, **28** (1989) 4531.
- 47 H.-J. Krüger and R. H. Holm, *Inorg. Chem.*, **27** (1988) 3645.
- 48 W. R. Pangratz, F. L. Urbach, P. R. Blum and S. C. Cummings, *Inorg. Nucl. Chem. Lett.*, **9** (1973) 1141.
- 49 R. M. C. Wei and S. C. Cummings, *Inorg. Nucl. Chem. Lett.*, **9** (1973) 43.
- 50 P. R. Blum, R. M. C. Wei and S. C. Cummings, *Inorg. Chem.*, **13** (1974) 450.
- 51 L. S. Chen and S. C. Cummings, *Inorg. Chem.*, **17** (1978) 2358.
- 52 M. F. Corringan and B. O. West, *Aust. J. Chem.*, **29** (1976) 1413.
- 53 I. Bertini, L. Sacconi and G. P. Speroni, *Inorg. Chem.*, **11** (1972) 1323.
- 54 K. Nag and D. S. Joardar, *Inorg. Chim. Acta*, **14** (1975) 433.
- 55 S. K. Mondal, P. Paul, R. Roy and K. Nag, *Transition Met. Chem.*, **9** (1984) 247.
- 56 S. K. Mondal, D. S. Joardar and K. Nag, *Inorg. Chem.*, **17** (1978) 191.
- 57 O. P. Anderson, J. Becher, H. Frydendahl, L. F. Taylor and H. Toftlund, *J. Chem. Soc., Chem. Commun.*, (1986) 699.
- 58 J. Becher, H. Toftlund and P. H. Oleson, *J. Chem. Soc., Chem. Commun.*, (1983) 740.
- 59 J. Becher, H. Toftlund, P. H. Oleson and H. Nissen, *Inorg. Chim. Acta*, **103** (1985) 167.
- 60 L. Casella, M. Gullotti and R. Vigano, *Inorg. Chim. Acta*, **124** (1986) 121.
- 61 L. Casella, M. Gullotti, A. Pintar, F. Pinciroli and R. Vigano, *J. Chem. Soc., Dalton Trans.* (1989) 1161.
- 62 M. Gullotti, L. Casella, A. Pintar, E. Suardi, P. Zanella and S. Mangani, *J. Chem. Soc., Dalton Trans.* (1989) 1979, and refs. therein.
- 63 L. Casella, *Inorg. Chem.*, **23** (1984) 2782, 4781.
- 64 P. Bordas, P. Sohar, G. Matolcsy and P. Berencsi, *J. Org. Chem.*, **37** (1972) 1727.
- 65 W. E. Blumberg and J. Piesach, *Biochim. Biophys. Acta*, **126** (1966) 269.
- 66 P. Beardwood and J. F. Gibson, *J. Chem. Soc., Chem. Commun.*, (1983) 1099.
- 67 Y. Murakami, Y. Matsuda and K. Sakata, *Inorg. Chem.*, **10** (1971) 1728, 1734.
- 68 A. L. Companion and M. A. Komarynski, *J. Chem. Educ.*, **41** (1964) 257.
- 69 A. W. Addison, *Inorg. Chim. Acta*, **162** (1989) 217.
- 70 R. Cammack, D. S. Patil, E. C. Hatchikian and V. M. Fernande, *Biochim. Biophys. Acta*, **98** (1987) 912.
- 71 D. L. Tennent and D. R. McMillin, *J. Am. Chem. Soc.*, **101** (1979) 2307.
- 72 V. Lum and H. B. Gray, *Isr. J. Chem.*, **21** (1981) 23.
- 73 H. R. Engeseth, D. R. McMillin and E. L. Ulric, *Inorg. Chim. Acta*, **67** (1982) 145.
- 74 J. A. Blaszak, E. L. Ulrich, J. L. Markley and D. R. McMillin, *Biochemistry*, **21** (1982) 6253.
- 75 L. Sacconi, *Transition Met. Chem.*, **4** (1968) 199.
- 76 S. C. Bhatia, J. M. Bindlish, A. R. Saini and P. C. Jain, *J. Chem. Soc., Dalton Trans.*, (1981) 1773.
- 77 M. A. Ali and S. E. Livingstone, *Coord. Chem. Rev.*, **13** (1974) 101.
- 78 G. A. Foulds, *Coord. Chem. Rev.*, **98** (1990) 1.
- 79 M. G. Kanatzidis, *Inorg. Chim. Acta*, **168** (1990) 101.
- 80 H.-J. Krüger and R. H. Holm, *Inorg. Chem.*, **28** (1989) 1148.
- 81 K. Osakada, T. Yamamoto, A. Yamamoto, A. Takenaka and Y. Sasada, *Acta Crystallogr., Sect. C*, **40** (1984) 85.
- 82 T. Yamamoto and Y. Sekine, *Inorg. Chim. Acta*, **83** (1984) 47.

- 83 D. H. Gerlach and R. H. Holm, *J. Am. Chem. Soc.*, *91* (1969) 3457.
- 84 G. W. Everett Jr., R. H. Holm and A. Chakravorty, *Prog. Inorg. Chem.*, *7* (1966) 83.
- 85 G. W. Everett Jr. and R. H. Holm, *Inorg. Chem.*, *7* (1968) 776.
- 86 G. W. Everett Jr. and R. H. Holm, *J. Am. Chem. Soc.*, *87* (1964) 2117.
- 87 R. H. Holm, *Acc. Chem. Res.*, *2* (1969) 307.
- 88 R. H. Holm, in G. N. LaMar, W. D. Horrocks and R. H. Holm, (eds.), *NMR of Paramagnetic Ions*, Academic Press, New York, NY, 1973, pp. 243–326.